The Role of Synthetic and Natural Fillers on Three-Body Abrasive Wear Behaviour of Glass Fabric–Epoxy Hybrid Composites

N. Mohan, S. Natarajan, S. P. KumareshBabu

Department of Metallurgical and Materials Engineering, National Institute of Technology, Tiruchirappalli – 620 015, India

Received 27 June 2010; accepted 23 April 2011
DOI 10.1002/app.34936
Published online 5 October 2011 in Wiley Online Library (wileyonlinelibrary.com).

ABSTRACT: Polymer matrix composites are a promising candidate in tribological applications due to possibility of tailoring their properties with special fillers. The comparative performance of Glass–Epoxy (G-E) composites with influence of synthetic fillers such as graphite (Gr) and silicon carbide (SiC) and biobased natural filler jatropha oil cake (JOC) was experimentally investigated. All the composites were fabricated using vacuum-assisted resin infusion (VARI) technique. The mechanical properties were studied in accordance with ASTM standards. The three-body abrasive wear studies were carried out with rubber wheel abrasion tester as per ASTM-G65 standard. Two different loads namely 22 N and 32 N with different abrading distances viz, 135, 270, 405, and 540 m are test parameters. The results reveal that addition of JOC in G-E composites has significant influence on wear under varied abrading distance/load. Further, it was found that SiC filled G-E composites exhibited better wear resistance compared to Gr/JOC filled G-E composites. The operating wear mechanisms have been studied by using scanning electron microscopy. © 2011 Wiley Periodicals, Inc. J Appl Polym Sci 124: 484–494, 2012

Key words: abrasive wear; glass fabric; epoxy; jatropha oil cake; graphite; silicon carbide; vacuum-assisted resin infusion technique; wear mechanism

INTRODUCTION

Polymers and their composites are extensively used in tribological application because of light weight, excellent strength to weight ratios, resistance to corrosion, non-toxicity, easy to fabricate, design flexibility, self lubricating properties, better coefficient of friction, and wear resistance. A few examples of components used in tribological applications are gears, cams, wheels, brakes, bearing liners, rollers, seals, clutches, bushings, transmission belts, pump handling industrial fluids, pipes carrying contaminated water, and chute liners abraded by coke.[1,2] Amongst the thermoset, epoxy resins are extensively studied as a matrix material for composite structures as well as adhesives for aerospace, automobile, and marine engineering applications because they exhibits low shrinkage, higher mechanical properties, easy fabrication, excellent chemical and moisture resistance, and good electrical characteristics.[3] Aramid/carbon fibers have good mechanical, thermal, and tribological properties than glass fibers, but the principal advantages of glass fibers are low cost with high strength. One of the challenges in the use of glass fiber-reinforced polymer (GFRP) composites for primary structures is to avoid the damage propagation during conditions involving abrasive wear.[4] The wear resistance of Polymer Matrix Composites (PMC's) can be enhanced by the reinforcing of filler materials such as graphite (Gr), molybdenum disulfide, and silicon carbide (SiC), etc. Gr and molybdenum disulfide provides self-lubrication property and SiC provides the hardness to the materials.[5] Incorporation of Gr particles in glass–epoxy (G-E) composites gives better mechanical properties and poor abrasive wear resistance and addition of SiC particles in G-E composite shows excellent mechanical properties and better tribological properties concluded by findings in the literatures.[6,7] Ray and Gnanamoorthy[8] found out fly ash filled vinylester resin matrix composites exhibit good wear resistance as compared to neat vinyl ester resin and exploited for various newer applications. Biswas and Satapathy[9] investigated wear behavior of red mud filled G-E composites. The red mud (an industrial waste generated during the production of alumina from Bauxite) filled glass fabric–epoxy composite shows better erosive wear properties as compared to unfilled G-E composite.

Natural mineral fillers such as talc, calcium carbonate, $BaSO_4$, organo clay, and fly ash filler

Correspondence to: S. Natarajan (drsnatarajan.nitt@gmail.com).

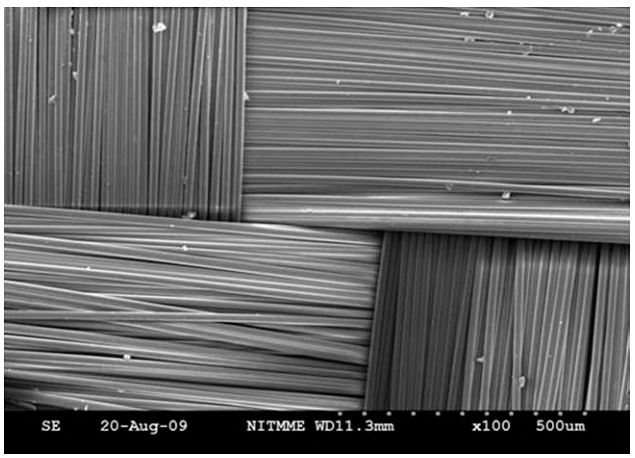

Figure 1 SEM image of dry glass fabric of diameter 18 μm.

addition in polymers make it as an alternative to metallic components in many of the general engineering application and tribological applications. The importance of tribological properties convinced many researchers to study the friction and wear behavior and to improve the wear resistance of polymeric composites. In light of the above, to improve the tribological behavior and enhance the load bearing capacity, glass fabric reinforcement is a good choice in natural filler filled epoxy matrix composites.[10,11]

Jatropha oil cake (JOC) is a by-product obtained after the mechanical extraction of oil from the jatropha seeds and glycerol is another by-product obtained after the transesterification of jatropha seed oil.[12] The JOC was found to contain 58% crude protein, 6.27% crude fiber, 6.57% acid detergent fiber, 8.71% neutral detergent fibers, and 0.18% acid detergent lignin. The reported higher ash content (9.82%) of JOC is an indication for the presence of large amounts of minerals which is an added reason to investigate this material for tribological applications.[13]

The coleus spent (CS) filled unsaturated polyester/polymethyl methacrylate (USP/PMMA) semi-interpenetrating polymer network (SIPN) composites showed better abrasion wear resistance as compared to unfilled SIPN system.[14] The sugarcane fiber reinforcement in the thermoset polymers had shown enhancing wear resistance.[15]

Recently, Mohan et al.[16,17] studied mechanical and two-body abrasive wear behavior of SiC and Gr particulate filled G-E composites. The filler filled G-E composite systems showed improved impact fracture toughness and better abrasive wear resistance as compared to unfilled G-E composites.

The natural fillers/fibres in the thermoset polymers exhibit good load bearing capacity and improved wear resistance.[18] Satheesh Kumar et al.[19] studied three-body abrasive wear behavior of natural and synthetic fillers in G-E composites and the wear performance of these composites in abrasive wear situations were in the sequence as follows: SiC-G-E>JOC-SiC-G-E>JOC-G-E>G-E. Gr is a solid lubricant and incorporation of Gr in G-E composites improves the mechanical and sliding wear behavior.[20] This research article aims at comparing the wear performance of synthetic and natural fillers in G-E composites and to explore the possibility of using bio-waste material JOC and thus opens new vistas to utilize locally available inexpensive natural jatropha waste product and produce a new candidate for tribo-material.

EXPERIMENTAL

Materials

E-Glass woven fabric 360 g/m^2 obtained from M/s. Reva Composites, Bangalore, India. The glass fabric diameters 18 μm was used as reinforcement are shown in Figure 1. Bifunctional epoxy-diglycidyl ether of butane diol (LY 5052) and cyclo aliphatic amine (HY 5052) (room temperature cure system) were obtained from M/s. HAM, Mumbai, India. The resin is a clear liquid, its viscosity at 25°C is 1000–1500 mPa and specific gravity is 1.17. The hardener is a liquid and its viscosity is 40–60 mPa and specific gravity is 0.94. The commercially available Gr powder was procured from M/s Libra Associates, Bangalore, India and SiC powder was obtained from M/s. Silicarb Recrystalized Pvt. Ltd., Bangalore, India. Its particle size ranged from 20 to 25 μm was used as filler material. JOC powder with particle size ranging from 50 to 70 μm was obtained from National University of Malaysia. It is obtained after extraction of oil from jatropha seeds; the obtained cake is dried and its powder was used as filler material (Fig. 2). The residual oil content present in the JOC was 3–7%.

Figure 2 Digital photo of jatropha oil cake. [Color figure can be viewed in the online issue, which is available at wileyonlinelibrary.com.]

Fabrication of composite specimen

The composite fabrication consist of six steps: (a) mixing of the epoxy resin and filler using a mechanical stirrer, (b) mixing of the curing agent with the filled epoxy resin, (c) fiber impregnation, (d) consolidation, and (e) curing of fabricated composites. In the first step (a), a known quantity of filler was mixed with epoxy resin using a high speed mechanical stirrer to ensure the proper dispersion of filler in the epoxy resin. In the second step (b), the hardener was mixed into the filled epoxy resin using a mechanical stirrer. The ratio of epoxy resin to hardener was 100 : 38 on weight basis. In the third step (c), composites were fabricated using the VARI process as described elsewhere.[21] Figure 3 shows schematic representation of VARI. Glass fabrics were cut into required dimensions. A granite mold was used for the fabrication. Granite mold was cleaned by using acetone and it is pre-coated with a releasing agent (suitable wax) to facilitate easier removal of the part from the mold. The glass fabrics are placed on a granite mold. On the top layer of the glass fabrics, a peel ply (porous teflon film) and breather were placed. This peel ply enables separation of the part from the vacuum bag and breather ensures uniform distribution of vacuum. A two sided insulated tape (acts as a sealant) was placed all around the fabrics at a distance of about 75 mm around the perimeter of the mold, an open spiral tubes were attached and connecting to a vacuum pump, which acts as a air channel from inside the mold when vacuum is applied. Air is evacuated by a vacuum pump and maintained at 0.0965 mPa of pressure, and a low viscosity epoxy resin is infused into the lay-up to impregnate the fabrics. In the fourth step (d), once the layers were wet with resin system, the vacuum bagging was removed. The entire assembly was again covered with vacuum bag with a new peel ply and breather and allowed to cure under vacuum at 0.0965 mPa of pressure at room temperature up to 24 h (Fig. 4). To improve the consolidation and reduce the voids and dry spots, the epoxy resin was injected into the mould surface before going into VARI. In the final step (e), the panels were post cured at 100°C for 3 h in a controlled oven. Flow chart of manufacturing process of hybrid composites is shown in Figure 5.

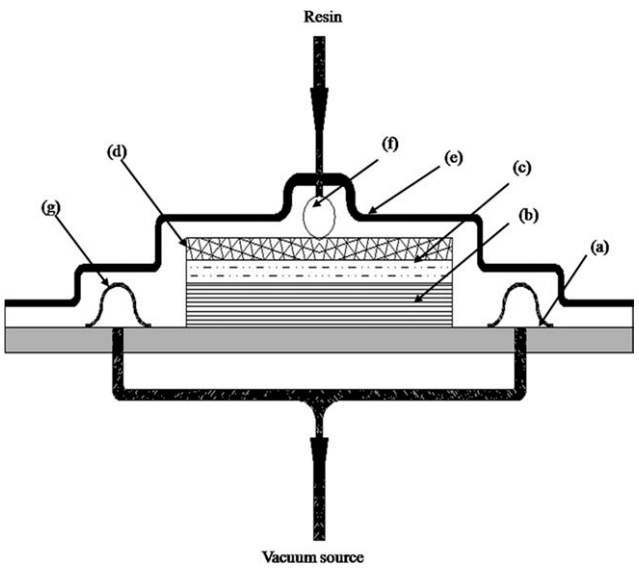

Figure 3 Schematic of VARI setup: (a) granite moulding tool, (b) dry glass fabrics, (c) peel ply and breather material, (d) distribution medium, (e) vacuum bag, (f) resin inlet, and (g) vacuum outlet.

Figure 4 Digital photo of vacuum bagging of series of G-E composites containing different fillers viz, Gr, SiC, and JOC. [Color figure can be viewed in the online issue, which is available at wileyonlinelibrary.com.]

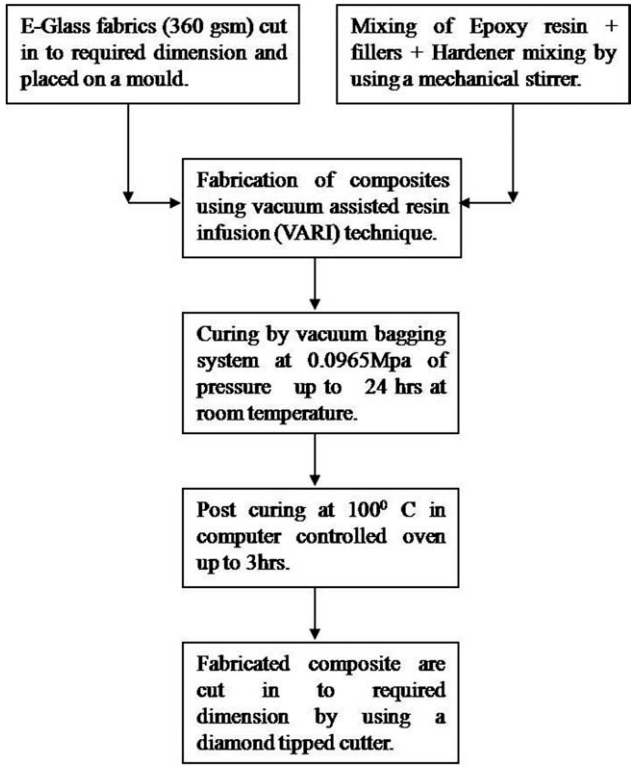

Figure 5 Typical flow chart of fabrication processing methodology of hybrid composites.

TABLE I
Formulations of Composites

Material (Designation)	Specimen code	Glass fiber (wt %)	Matrix (wt %)	Filler (wt %)
Glass fabric-epoxy composite	G-E	60	40	–
Silicon carbide filled glass fabric–epoxy composite	SiC-G-E	60	34	6
Graphite filled glass fabric–epoxy composite	Gr-G-E	60	34	6
Graphite & JOC filled glass fabric–epoxy composite	Gr-JOC-G-E	60	34	6
JOC filled glass fabric–epoxy composite	JOC-G-E	60	34	6

The glass fiber : matrix (epoxy) : filler ratio was 60 : 36 : 6. The unfilled G-E composites were designated as G-E, SiC filled G-E composites as SiC-G-E, Gr filled G-E composites as Gr-G-E, Gr + JOC filled G-E composite as Gr-JOC-G-E, and JOC filled G-E composites as JOC-G-E. The details of the composites are provided in Table I. The laminate of dimensions 300 mm × 300 mm × 2.6 ± 0.2 mm was fabricated, the specimens for the required dimensions were cut using a diamond tipped cutter. Density of the composite specimens was determined using a high precision digital electronic weighing balance of 0.1 mg accuracy by using Archimedes principle.

Techniques

The tensile behavior of composites specimens (Fig. 6) were evaluated with an Instron universal testing machine (1–100 kN, UK series IX automated material testing system) as per ASTM D 3039. The test was conducted at a cross-head speed of 10 mm/min. The surface hardness of the composite was measured using shore-D durometer (M/s. PSI Sales Pvt. Ltd., India) as per ASTM D 2240.

The modified dry sand/rubber wheel abrasion test set up as per ASTM G-65 was used to conduct the three-body abrasive wear experiments (Fig. 7). The surface of the specimen is cleaned with a soft paper soaked in acetone before the test. The specimen weight is recorded using a digital electronic balance (0.1 mg accuracy) before it was mounted in the specimen holder. The difference between initial and final weight of the specimen was a measure of abrasive wear loss. A minimum of three trials were conducted to ensure repeatability of test data. The silica sand of angular in shape with a grain size 53–75 μm was used as abrasives in this study (Fig. 8). The abrasive was fed at the contacting face between the rotating rubber wheel and test specimen. The tests were conducted at a rotational speed of 200 rpm. The rate of feeding the abrasive was 250 ± 10 g/min. The experiments were carried out for loads of 22 N and 32 N and at a constant rubbing velocity of 2.33 m/s. Further, the abrading distances were varied in steps of 135 m from 135 to 540 m. The wear behavior was measured by the loss in weight, which was then converted into wear volume using the measured density data. The specific wear rate (K_s) was calculated from the equation;

$$K_s = \frac{\Delta V}{L \times d}\ \mathrm{m^3/Nm} \quad (1)$$

where, ΔV is the volume loss in m^3, L is the load in Newton, and d is the abrading distance in meters.

Figure 6 Digital photo of series of G-E composite tensile specimens containing different fillers viz, SiC, Gr, and JOC as per ASTM standard. [Color figure can be viewed in the online issue, which is available at wileyonlinelibrary.com.]

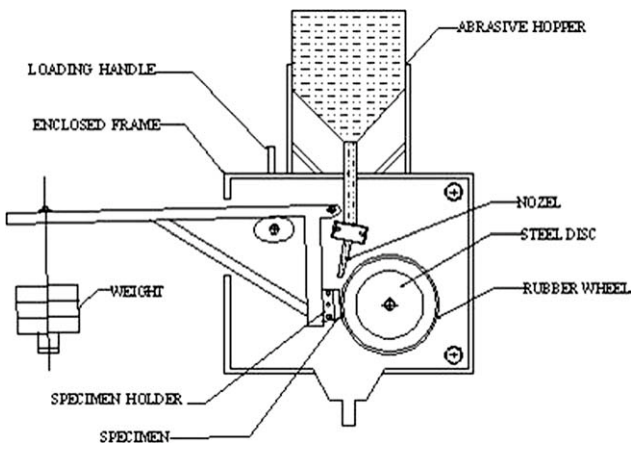

Figure 7 A shematic diagram of dry sand rubber wheel abrasive wear machine.

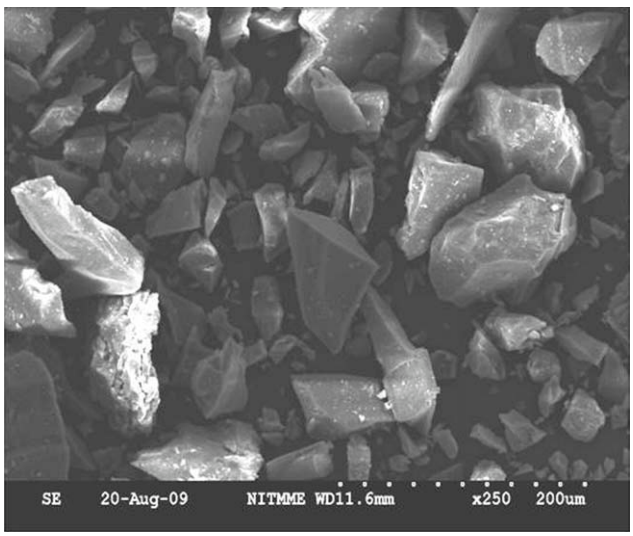

Figure 8 SEM image of the silica sand abrasives used for testing.

RESULTS AND DISCUSSION

Mechanical properties

The mechanical properties of filled and unfilled G-E composites are mentioned in Table II. A comparison of the result reveals that filler-filled composite system shows better tensile strength and higher hardness value. The mechanical properties depend to a greater extent on the reinforcement/filler and to a lesser extent on the matrix material and interface interaction between them. The correlation between wear volume loss and (σe) factor ("σ" is ultimate tensile strength and "e" is ultimate elongation) has been reported in the literature.[7] In general, the incorporation of fiber/filler increases the tensile strength (σ) and reduces the ultimate elongation (e). Hence, the product σe may become smaller in the case of a filled system compared to an unfilled system. In the present study, amongst the series of composites, the SiC filled G-E composite has the highest wear resistance and lowest (σe) factor. The highest and lowest hardness was noted for SiC and JOC filled G-E composites, respectively. This is due to the fact that SiC comprises tetrahedral crystals of carbon and silicon atoms with strong bonds in the lattice. This exhibits a very hard and strong material reinforcement with excellent dimensional stability. During abrasive actions, hardness of the material play a major role in improving the wear resistance of the composite.[22] The soft and elastomeric nature of natural JOC filled G-E composite show slightly higher tensile strength and higher elongation at fracture than unfilled G-E composite. As compared to JOC filled composite, Gr and Gr + JOC filled G-E composite exhibits slightly higher tensile strength and lower elongation at fracture. This is due to atomic structure of Gr which enhances the tensile behavior of the composite.

Wear loss and specific wear rate

The plot of wear volume loss as a function of abrading distance is shown in Figure 9(a,b), respectively. When hard silica sand particles abrade the composite specimen surface under applied load it produces groove. Figure 9(a,b) indicates wear loss increases with increase in abrading distance/applied load. This is due to energy barrier created at the junction of the surface. At lower loads, the energy generated by abrasive particles is not sufficient to break the surface energy barrier, i.e., difficult to penetrate into the surface due to the resistance provided in the form of surface energy by the composite sample, whereas at higher loads, particles gain energy from the high speed rubber wheel, hence high wear volume loss was observed. In case of filler-filled G-E composite, wear loss increases with the increase in applied load. Energy barrier created at the surface is greater due to the reinforcement of hard filler particles into the matrix. Hence at even higher loads, energy generated by abrasive particles is not sufficient. As a result, abrasive particles cannot get penetrated deeper into the matrix material. The gained energy from the high speed rubber wheel is sufficient for microcutting of large amount of glass

TABLE II
Mechanical Properties of Various Filler Filled Composites

Properties	G-E	SiC-G-E	Gr-G-E	Gr-JOC-G-E	JOC-G-E
Tensile strength (MPa) (σ)	309	342	320	319	311
Standard deviation	2.77	4.33	3.84	3.43	3.39
Tensile modulus (GPa)	16.22	18.66	19.12	18.54	18.61
Standard deviation	0.14	0.23	0.22	0.19	0.20
Elongation at fracture (%) (e)	3.8	3.5	3.3	3.8	3.9
Standard deviation	0.24	0.20	0.15	0.31	0.35
Product (σe)	1174	1197	1056	1212	1213
$1/(\sigma e)$ factor ($\times 10^{-4}$)	8.51	8.35	9.45	8.25	8.24
Surface hardness (Shore-D)	85	91	88	86	80
Standard deviation	1.30	2.30	2.07	1.92	1.22
Density (g/cc)	1.78	1.80	1.79	1.76	1.70

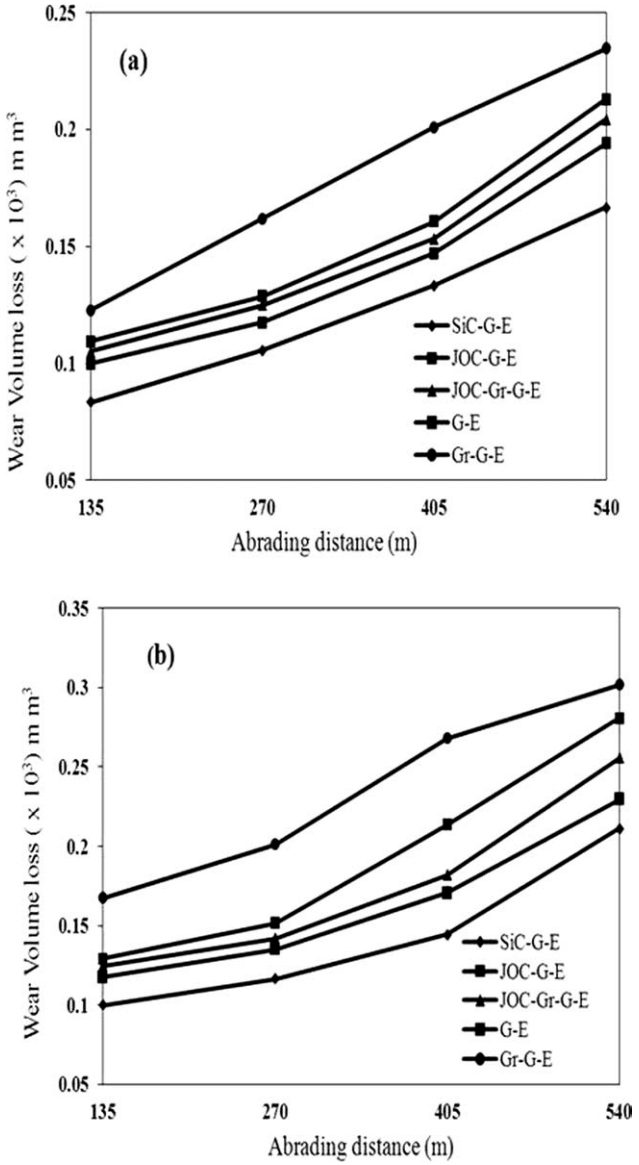

Figure 9 Effect of abrading distances on wear volume loss of composites at (a) 22 N and (b) 32 N load.

fibres.[23,24] Hence, similar observations are found in the present investigation. A lowest wear volume loss of 0.1 × 10^3 mm^3 was observed for SiC-G-E composite and highest wear loss of 0.3 × 10^3 mm^3 was noticed for Gr filled composite at a load of 32 N. As compared to unfilled G-E composite, the SiC filled G-E composite exhibit high wear resistance. However, Gr filled G-E composite has shown the highest wear volume loss even though the factor σ*e* magnitude is almost same as G-E composite. This is also evident from the wear mechanism studies of Gr filled composite from the photo micrograph in Figure 13. This may be attributed to the poor interfacial adhesion of the Gr in G-E composite which gives rise to the increased wear rate. The wear data of the composites reveal that the wear behavior strongly depends on the operating parameters. The influence of fibers/fillers on the abrasive wear resistance of clean polymer is more complex and unpredictable and mixed trends are reported.[6] As compared to Gr-G-E, JOC-Gr-G-E, and G-E composites JOC-G-E composite shows better wear resistance and progressive wear volume loss due to presence of rich minerals and ash in JOC, which moderates friction co-efficient during abrasion action. Hence the hard silica particles slip/slide on the specimen surface and JOC in matrix act as a good anti-wear additive. In SiC filled G-E composite, abrading distance was the major contributing factor. As the abrading distance increases, the hard SiC particles and glass fiber resist the penetration of abrasive particles into the composite. Finally, when the SiC particles are pulled due

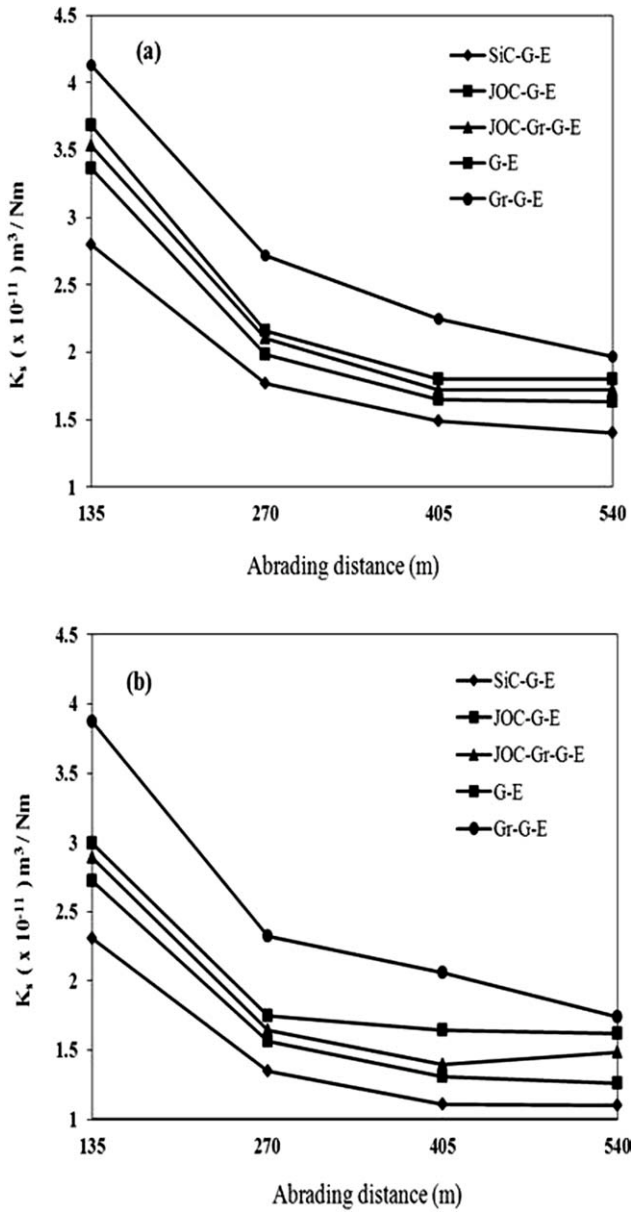

Figure 10 Specific wear rate as a function of abrading distances of composites at (a) 22 N and (b) 32 N load.

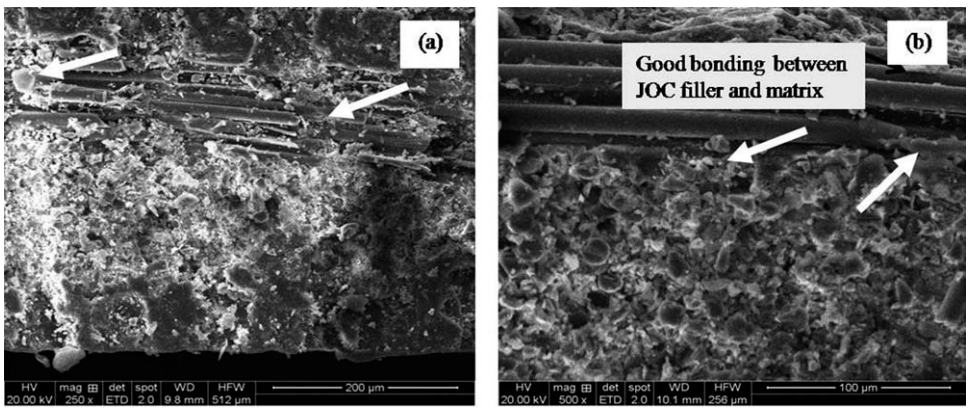

Figure 11 SEM images of cross-section of JOC-G-E composites (a) 250× and (b) 500× (magnification)

to continuous action, the matrix layer is removed resulting in the formation of a groove. Subsequently, glass fibers are subjected to action along with SiC particles, which provides additional abrasive wear resistance. Hence there was an improved abrasive wear resistance of the SiC filled composite.[24] The presence of Gr and JOC in G-E composite system gives better wear resistance as compared to unfilled and Gr filled composites. This is due to the mixture of natural and synthetic filler in G-E composite which gives combined effects on both mechanical properties and wear performance.

The wear resistance offered by different composites of the present investigation is as follows: SiC-G-E> JOC-G-E>JOC-Gr-G-E>G-E>Gr-G-E for the two different loads (22 N and 32 N). At this juncture, the authors are pleased to quote the research work of Zhang and coworkers,[25–28] which confirm that hybrid composites have considerable wear resistance.

The plot of specific wear rate (K_s) as a function of abrading distance is shown in Figure 10(a,b), respectively. The specific wear rate significantly decreases with increase in abrading distance and applied load on the composite specimen. A highest specific wear rate of 4.13×10^{-11} m^3/Nm is observed for Gr-G-E composite and a lowest specific wear rate of 1.1×10^{-11} m^3/Nm is observed for SiC-G-E composite. The specific wear rate for Gr filled G-E composite lies in the range of 4.13×10^{-11} m^3/Nm to 1.74×10^{-11} m^3/Nm, unfilled G-E composite lies in the range of 3.68×10^{-11} m^3/Nm to 1.62×10^{-11} m^3/Nm, JOC-Gr filled G-E composite lies in the rage of 3.53×10^{-11} m^3/Nm to 1.48×10^{-11} m^3/Nm, and JOC-filled G-E composite lies in the range of 3.36×10^{-11} m^3/Nm to 1.26×10^{-11} m^3/Nm. As compared to Gr-G-E, JOC-Gr-GE, and G-E composite lower value of specific wear rate was noticed for JOC-filled and SiC filled G-E composite. The presence of rich ash, minerals, and protein content in JOC act as flexible filler and have a good dispersion with matrix and reduces the void content in epoxy, hence improves the wear resistance (Fig. 11 shows cross-section image of JOC-G-E composites and a white arrow mark indicates good bonding between fiber and matrix).

From Figure 10 it was noticed that at lower abrading distances (135–270 m) a drastic reduction in specific wear rate and with further increase in abrding distance from 270 m to 540 m, a linear reduction of specific wear rate was observed for all the composite specimen. This can be attributed to the fact that at

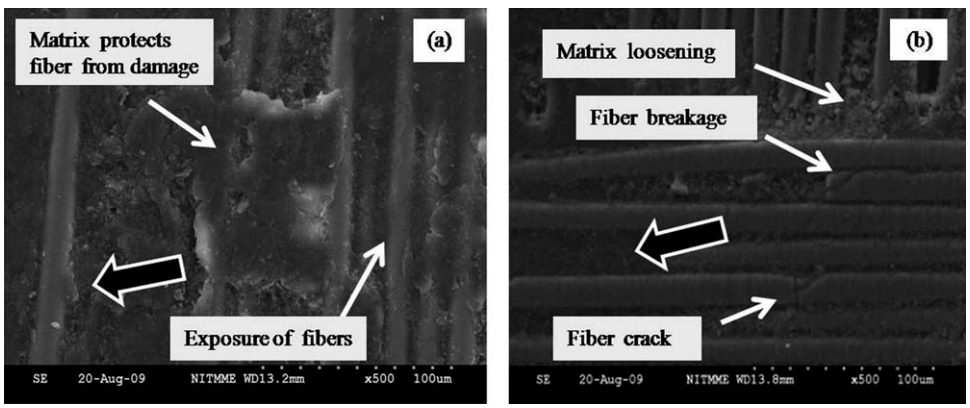

Figure 12 SEM images of unfilled G-E composite at 32 N load, (a) 135 m and (b) 540 m abrading distance.

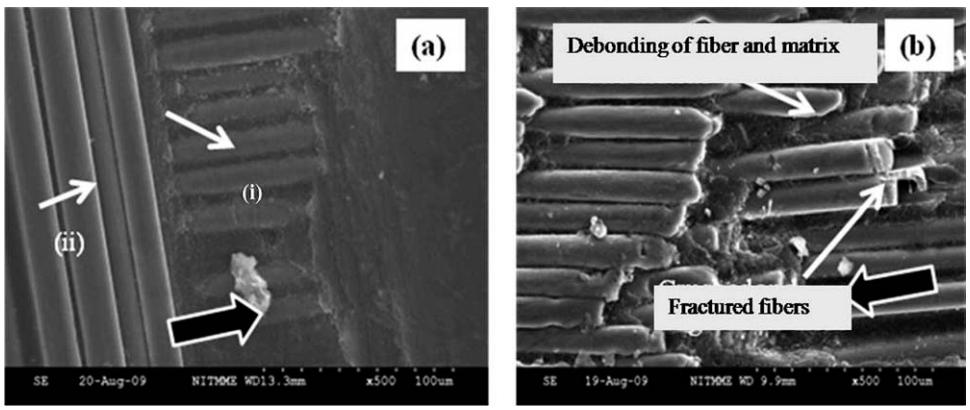

Figure 13 SEM images of Gr filled G-E composite at 32 N load, (a) 135 m and (b) 540 m abrading distance.

lower abrading distance, low modulus polymer matrix (soft component) was exposed to abrasion, which is less hard as compared to silica sand and hence high specific wear rate resulting in matrix damage and less exposure of fibre as shown in SEM images [Figs. 12(a)–16(a)].

At higher abrading distance, high modulus glass fabric was exposed to abrasion,which show both low and steady-state wear rate. Thus, the rate at which the material removed with respect to abrading distance decreases. This is because higher hardness provides better resistance against abrasion and in turn, abrasive particles have to work more to facilitate failure, i.e., much higher amount of energy to facilitate fibre failure. The behaviour can be explained from the concept of conservation of energy and its exchange within the composite specimen. Similar observations were noticed by Chand et al. [23] and Unal et al.[29] in their study of abrasive wear of polymeric materials.

WORN SURFACE MORPHOLOGY

The worn surface features of the composites were examined using a scanning electron microscope (SEM). The SEM features of the worn surfaces of filled and unfilled G-E composites at 32 N load at two abrading distances (135 and 540 m) are shown in Figures 12–16. For the sake of clarity the direction of abrasion (big arrow) is shown on SEM images.

The surface features of unfilled G-E composite worn surfaces are shown in Figure 12(a,b). Figure 12(a) shows that epoxy matrix protects the fiber from damage and exposure of longitudinal fibers in the direction perpendicular to the abrasion. Figure 12(b) depicts exposure of both longitudinal and transverse fibers and a detachment of matrix in between the fibers and brakeage of fibers.

Gr-G-E composites (Fig. 13) show more fiber cutting and the fiber ends have an appearance of chipped out in features. From Figure 13(a) it is noticed that a layer of longitudinal fiber was eroded (marked as (i)) and exposure of longitudinal fibers (marked as (ii)) and also parting up off abraded and un-abraded surface Figure 13(b) indicates exposure of transverse fibers including severe fiber damage due to detachment of matrix from fiber and loosening of Gr filler. Further, fractured fibers and interfacial debonding were noticed. The interfacial debonding results into more and more naked fibers, which

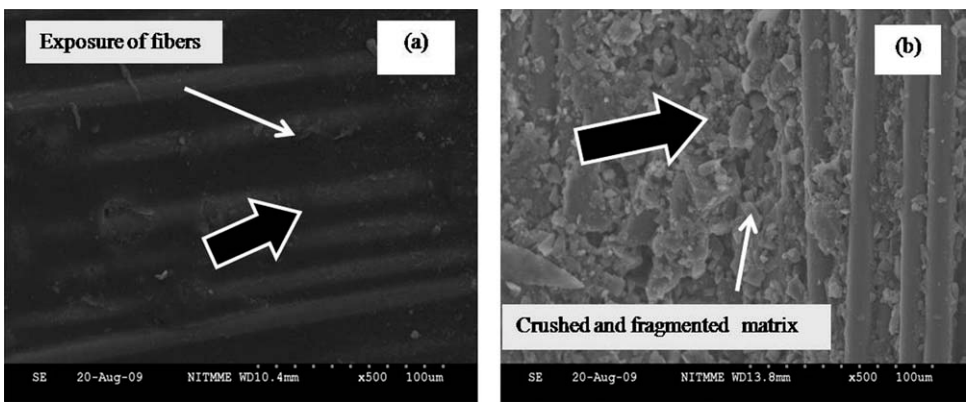

Figure 14 SEM images of Gr+JOC filled G-E composite at 32 N load, (a) 135 m and (b) 540 m abrading distance.

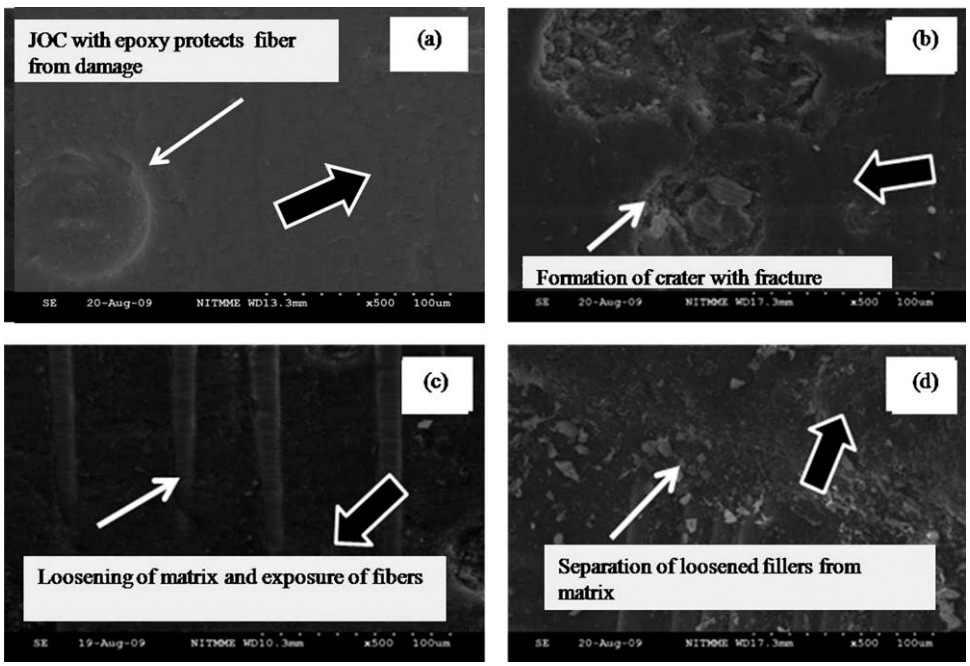

Figure 15 SEM images of JOC filled G-E composite at 32 N load, (a) 135 m, (b) 270 m, (c) 405 m, and (d) 540 m abrading distance.

are exposed to the abrasive medium. As compared to unfilled composite the Gr-filled composite show more fiber fracture and matrix wear. The characteristic feature of the Gr-G-E composite is the presence of Gr filler in form of particulate. In these SEM images, severe matrix failure is observed because Gr filler, due to their porous nature absorbs the resin during composite preparation, hence less fiber and matrix interaction has been observed.

The worn surface features of Gr/JOC filled G-E composite at 32 N loads are shown in Figure 14. It is noticed that at lower abrading distance (Fig. 14a), matrix damage and matrix removal due to the propagation of micro and macro cracks on the surface. The main features observed are matrix wear leading to exposure of transverse fibers to the abrasion direction. In Figure 14(b), at higher abrading distance, matrix is distorted and damaged by ploughing and cutting action by sharp abrasive particles and exposure of few longitudinal fibers without damage. This is due to the presence of JOC and Gr in epoxy matrix acts as a good interfacial adhesion. The exposed fibers show good adhesion with the matrix and no damage of fibers are observed. As compared to Gr-G-E composite and unfilled G-E composite system in Gr-JOC-G-E composite shows less damage of fiber and matrix and worn surfaces are relatively smooth.

Figure 15 indicates worn out surfaces fetures of JOC filled composite at 32 N load and at different

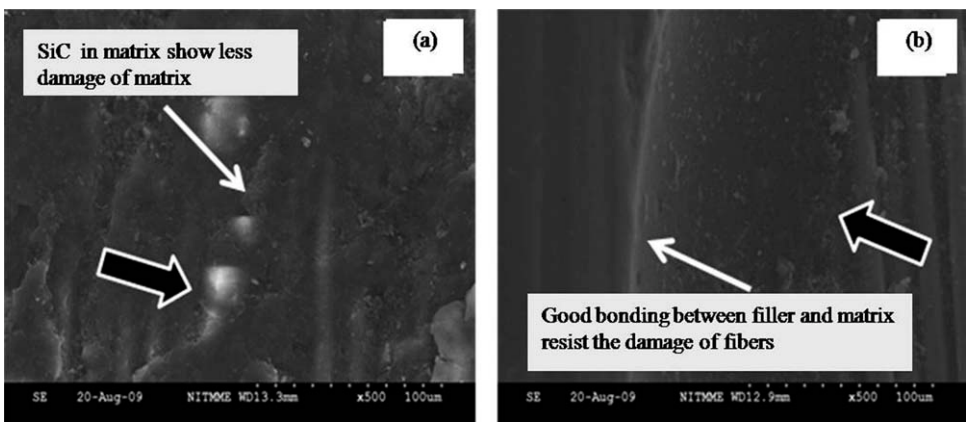

Figure 16 SEM images of SiC filled G-E composite at 32 N load, (a) 135 m and (b) 540 m abrading distance.

abrading distances viz, 135, 270, 405, and 540 m. The SEM image of lower abrading distance (135 m), [Fig. 15(a)] indicates enveloping of fibre by JOC with epoxy and protects both matrix and fibre damage during abraison. With the increse in abrading distance [(270 m, Fig. 15(b)] formation and development of crater with multiple fractures was observecd. In Figure 15(c) (at 405 m), a losening of matrix and exposure of few longitudinal fibres were noticed. At higher abrading distance [540 m, Fig. 15(d)] matrix wear, exposure of longitudinal fibre in the direction parallel to the abrasion and separation of loosened filler and matrix were observed. As compared to Gr-G-E, Gr-JOC-G-E composite and unfilled G-E composite in JOC-G-E composite shows less damage of fiber and matrix.

Figure 16(a,b) shows the worn out surface feature of SiC filled G-E composites at 135 m and 540 m abrading distances at 32 N load. At lower abrading distances in Figure 16(a), SiC particles containing the epoxy matrix present on the surface of the composite are inferred to act as an effective barrier to prevent the large scale fragmentation. At higher abrading distance [Fig. 16(b)], a good interfacial bonding between filler and matrix exist that resists the damage of the fibre.

A significant difference between the SEM images of unfilled and filled G-E composite could be observed. Both at high and low abrading distances, the SiC filled G-E composite (Fig. 16) exhibited relatively less damage of matrix and fiber compared to the unfilled, JOC filled, and Gr filled G-E composite. From the SEM image of G-E composite containing JOC (Fig. 15), it is observed that a very low fragmentation of matrix and fibers. This could be reason for better improvement in abrasion resistance. The excellent improvement in the abrasion resistance was observed in SiC filled G-E composite compared to Gr filled, JOC filled, and unfilled G-E composite. This is due to SiC in G-E composite that exhibits a good adhesion between the fiber matrix interface.

CONCLUSIONS

From three-body abrasive wear studies of unfilled and filled G-E composites following conclusions can be drawn:

- Tribological behavior of unfilled and filler filled G-E composites strongly depends on the experimental test parameters such as abrading distance and applied load.
- The specific wear rate in the initial stage was very high and as the abrading distance increased, it decreased gradually and reached steady state.
- The energy transfer concept was applied to explain the mechanism of material removal in the composite.
- Among the three fillers employed, SiC filled G-E composite shows better excellent abrasion resistance.
- Fairly poor correlations between tribological properties and mechanical properties observed for Gr filled and unfilled G-E composite system.
- A mixture of natural JOC and synthetic Gr in G-E composites gives synergistic effect on both mechanical properties and wear performance.
- SEM studies on worn surfaces indicate the involvement presence of crushed and fragmented fibers, fragmentation of matrix and fiber, formation of crater and development of crater wear, parting up of surface, separation/removal of filler from the matrix.

The authors wish to express their gratitude for the provision of the excellent experimental facilities, established under TEQIP in the Department of Metallurgical and Materials Engineering, National Institute of Technology, Tiruchirappalli. One of the author (N. Mohan) is grateful to the management and principal of Dr. Ambedkar Institute of Technology, Bangalore, and AICTE New Delhi for their help and valuable support during the course of this work.

References

1. Sampathkumaran, P.; Seetharamu, S.; Vynatheya, S.; Murali, S.; Kumar, R. K. Wear 2000, 237, 20.
2. Pihtili, H.; Tosun, N. Compos Sci Technol 2002, 62, 367.
3. Deng, S.; Ye, L.; Friedrich, K. J Mater Sci 2007, 42, 2766.
4. Bijwe, J.; Awtade, S.; Ghosh, A. Wear 2006, 260, 401.
5. Bijwe, J.; Rajesh, J.; Jeyakumar, J.; Ghosh, A.; Tewari, U. S. Tribol Int 2000, 33, 697.
6. Suresha, B.; Chandramohan, G.; Siddaramaiah; Jayaraju, T. J Polym Compos 2008, 29, 1028.
7. Suresha, B.; Chandramohan, G.; Kishore, P.; Sampathkumaran, S.; Seetharamu, S. Polym Compos 2008, 29, 631.
8. Ray, D.; Gnanamoorthy, R. J Reinforced Plast Comp 2007, 26, 5.
9. Biswas, S.; Satapathy, A. Mater Design 2009, 30, 2841.
10. Dasari, A.; Yu, Z.-Z.; Mai, Y.-W.; Hu, G.-H.; Varlet, J. Compo Sci Technol 2005, 65, 2314.
11. Yilmaz, M. G.; Unal, H.; Mimaroglu, A. Express Polym Lett 2008, 2, 890.
12. Satheesh Kumar, M. N.; Yaakob, Z.; Abdulla, R. S. Recent Pat Mater Sci 2009, 2, 131.
13. Makkar, H. P. S.; Francis, G.; Becker, K. J Sci Food Agric 2008, 88, 1542.
14. Syed, M. Z.; Siddaramaiah; Suresha. B.; Syed. A. A. J Compos Mater 2009, 43, 2387.
15. El-Tayeb, N. S. M. Wear 2008, 265, 223.
16. Mohan, N.; Natarajan, S.; Kumaresh Babu, S. P.; Siddaramaiah. J Miner Mater Charact Eng 2010, 9, 231.
17. Mohan, N.; Natarajan, S.; Kumaresh Babu, S. P. Int J Mater Sci 2010, 5, 181.
18. Mohan, N.; Natarajan, S.; Kumaresh Babu, S. P.; Siddaramaiah. J Am Oil Chem Soc 2011, 88, 111.

19. Satheesh Kumar, M. N.; Yaakob, Z.; Mohan, N.; Siddaramaiah; Kumaresh Babu, S. P. J Am Oil Chem Soc 2010, 87, 929.
20. Suresha, B.; Chandramohan, G.; Renukappa, N. M.; Siddaramaiah. J Appl Polym Sci 2007, 103, 2472.
21. Chisholm, N.; Mahfuzi, H.; Rangari, V.; Rodgers, R.; Jeelani, S. NSTI-Nanotechnol 2004, 3, 302.
22. Harsha, A. P.; Tewari, U. S.; Venkatraman, B. Wear 2003, 254, 680.
23. Chand, N.; Naik, A.; Neogi, S. Wear 2000, 242, 38.
24. Basavarajappa, S.; Joshi, A. G.; Arun, K. V.; Praveen Kumar, A.; Prasanna Kumar, M. J Polym Plast Technol Eng. 2010, 49, 8.
25. Su, F.-H.; Zhang, Z.-Z.; Liu, W.-M. Wear 2006, 260, 861
26. Su, F.-H.; Zhang, Z.-Z.; Liu, W.-M. Compos Sci Technol 2007, 67, 102.
27. Su, F.-H.; Zhang, Z.-Z.; Liu, W.-M. Wear 2008, 264, 562.
28. Feng, H. S.; Zhao, Z. Z. J Appl Polym Sci 2009, 112, 594.
29. Unal, H.; Sen, U., Mimaroglu, A. Mater Design 2005, 26, 705.